Observation of Anisotropy in Thermal Conductivity of Individual Single-Crystalline Bismuth Nanowires

Jong Wook Roh,[†,#] Kedar Hippalgaonkar,[‡,#] Jin Hee Ham,[†] Renkun Chen,[§] Ming Zhi Li,[‡] Peter Ercius,[⊥] Arun Majumdar,[‡,△] Woochul Kim,[∥,*] and Wooyoung Lee[†,*]

[†]Department of Materials Science and Engineering, Yonsei University, 262 Seongsanno, Seoul 120-749, Korea, [‡]Department of Mechanical Engineering, University of California, Berkeley, California 94720, United States , [§]Department of Mechanical and Aerospace Engineering, University of California, San Diego 92093, United States, [⊥]National Center for Electron Microscopy, Lawrence Berkeley Laboratories, Berkeley, California 94720, United States , and [∥]School of Mechanical Engineering, Yonsei University, 262 Seongsanno, Seoul 120-749, Korea. [#] These authors contributed equally to this work. [△] Present address: Advanced Research Projects Agency-Energy (ARPA-E), U.S. Department of Energy, Washington, DC 20585, United States.

ABSTRACT The thermal conductivity of individual single-crystalline Bi nanowires grown by the on-film formation of nanowires (ON–OFF) has been investigated. We observed that the thermal conductivity of single-crystalline Bi nanowires is highly anisotropic. Thermal conductivity of nanowires (diameter ~100 nm) in the off-axis [$\bar{1}$02] and [110] directions exhibits a difference of ~7.0 W/m·K. The thermal conductivity in both growth directions is diameter-dependent, which indicates that thermal transport through the individual Bi nanowires is limited by boundary scattering of both electrons and phonons. This huge anisotropy in thermal conductivities of Bi nanowires suggests the importance of direction-dependent characterization of charge, thermal transport, and thermoelectric properties of Bi nanowires.

KEYWORDS: bismuth · nanowires · anisotropy · thermal conductivity · size effect

Bismuth (Bi), which is a semimetal with a rhombohedral crystal structure and highly anisotropic Fermi surface,[1−3] has attracted great attention due to its unique transport properties such as anisotropic carrier transport,[1] bipolar electrical resistivity,[4] and low carrier effective masses,[5] revealed by earlier research on the Seebeck coefficient,[6] galvanomagnetic effects,[4] de Haas–Van Alphen effects,[7] and cyclotron resonance.[5,8] Furthermore, electrical measurements on Bi nanowires have thrown light on the semimetal-to-semiconductor transition below a diameter of the Bohr radius of Bi (~50 nm).[9,10] However, few direct measurements of thermal conductivity of Bi have been performed, which has a strong interplay between electrons, holes, and phonons as heat carriers. In semimetallic Bi, the electronic contribution is significant to thermal conductance from 100 to 300 K, while the phonons contribute almost exclusively to thermal conductance below 50 K.[1,11] Also, most electrical and thermal transport properties of bulk Bi have been understood in terms of the trigonal (parallel) and three equivalent binary (perpendicular) crystal orientations. This directional-dependent behavior not only gives the electrons and holes different effective masses but also results in a distinction in the speed of sound.[12] The fundamental understanding of the carrier scattering in Bi can be furthered by tailoring the geometries of Bi to impede phonon and electronic carriers, as well as tune the band structure based on quantum confinement effect.[9,10,13] In particular, these would be very useful to enhance the power factor ($S^2\sigma$), where S is the Seebeck coefficient and σ is the electrical conductivity, and/or decrease the thermal conductivity, κ, for thermoelectric applications.[13,14]

The efficiency of thermoelectric devices is quantified by the thermoelectric figure of merit (ZT) of a given material, which is defined as $ZT = S^2\sigma T/\kappa$. Single-crystalline Bi nanowires have been of great importance due to the expected quantum confinement effect, which should enhance the power factor without significantly affecting κ.[15,16] In prior work, it was shown that high-quality single-crystalline Bi nanowires grown by the on-film formation of nanowires (OFF–ON)[17] have very large electronic mean free paths ($\lambda_e \approx 1.35\ \mu$m), which are about an order of magnitude higher than bulk.[1] This arises due to a reduction of the Fermi energy, E_F, with the diameter of the nanowires (d_w).[17] The mean free path of phonons at 300 K can be estimated to be about 11–14 nm on the basis of the Dulong–Petit limit, and $l \approx 3\kappa/(C_v \times \nu)$,[11] where κ is the measured thermal conductivity of bulk Bi (about 8–10 W/m·K), C_v is the volumetric specific heat of bismuth (about 1.2 J/cm^3·K),

* Address correspondence to wooyoung@yonsei.ac.kr; woochul@yonsei.ac.kr.

Received for review February 5, 2011 and accepted April 5, 2011.

Published online April 05, 2011
10.1021/nn200474d

and v is the speed of sound (~1790 m/s).[11] Thus, nanowires of diameters close to the mean free path can effectively scatter both phonons and electrons. So far, only a few studies have been conducted on thermal transport in Bi nanowires. Heremans *et al.*[18] investigated the thermal conductance of Bi nanowires embedded in anodic alumina, *e.g.*, Bi nanowire/alumina template composite. Moore *et al.*[19] studied thermal conductivity of individual Bi nanowires grown by the vapor deposition method. They demonstrated thermal conductivity suppression in Bi nanowires compared with bulk Bi, yet most of their study was performed on polycrystalline Bi nanowires with the exception of one single-crystalline Bi nanowire. Furthermore, it should be noted that the thermal conductivity of bulk Bi is highly anisotropic.[1] In this study, we perform the first systematic study on the thermal conductivity of individual single-crystalline Bi nanowires with various diameters and different crystal orientations, thus throwing some light on the transport mechanism in this prospective high-efficiency thermoelectric material.

RESULTS AND DISCUSSION

OFF–ON, a stress-induced method for growing high-quality single-crystalline nanowires, was employed in this work to grow single-crystalline Bi nanowires.[17] Since detailed growth mechanisms are available in refs 17 and 20, only a brief explanation is provided here. A Bi thin film was deposited onto a thermally oxidized Si(100) substrate using an ultrahigh vacuum (UHV) radio frequency (rf) sputtering system with a base pressure of 4×10^{-8} Torr. After heat treatment of the as-grown Bi thin film at 270 °C for 10 h, Bi nanowires were extruded from the surface of the as-grown Bi film. This spontaneous growth of Bi nanowires is attributed to the substantial atomic diffusion to relax compressive stress on the as-grown Bi film. This originates from the mismatch of thermal expansion coefficient between Bi films and the SiO_2/Si substrate during heat treatment, as illustrated in Figure 1a.[17] As shown in Figure 1b, Bi nanowires grown by OFF–ON were found to be uniform in diameter, with aspect ratios exceeding 1000. A high-resolution transmission electron microscopy (HR-TEM) image and a corresponding selected area electron diffraction (SAED) pattern demonstrate that the Bi nanowires are single-crystalline with a growth direction of [110] and [$\bar{1}$02], as shown in Figure 1c and d, respectively. On the basis of this method, other thermoelectric materials, such as Bi,[17] Bi_2Te_3,[20] BiSb, and Bi_2Se_3 nanowires, could also be produced in single-crystalline phase.

Suspended microdevices were employed in measuring the thermal conductivity of individual Bi nanowires. A detailed description of thermal conductivity measurement based on these devices is available in the literature,[21–24] so only a brief explanation is provided here. Figure 2a shows a field emission scanning electron microscopy (FE-SEM) image of a suspended microdevice that consists of two silicon nitride (SiN_x) membranes suspended with five supporting SiN_x beams each. Pt resistance thermometer (PRT) coils with a width of 1 μm and a thickness of 50 nm on each SiN_x membrane were utilized as both heater to increase the temperature of the heating membrane and as a thermometer to measure the temperature on both heating and sensing sides. After placing the individual Bi nanowires between the two SiN_x membranes using either a drop-casting method or nanomanipulation, a Pt/C composite was deposited locally to improve the thermal contact between the Bi nanowire and membrane using the electron beam of a dual-beam focused ion beam (FIB) system (FEI Quanta 3D FEG), as shown in Figure 2b. All thermal conductivity (κ) measurements were carried out in a high vacuum of less than 5.0×10^{-6} Torr in order to eliminate convection heat losses. The thermal conductivity was extracted using $\kappa = G_w l/A$ from a measured thermal conductance through the individual Bi nanowires (G_w), where l is the length between the thermal contacts deposited on each membrane and A is the cross-sectional area of a nanowire.

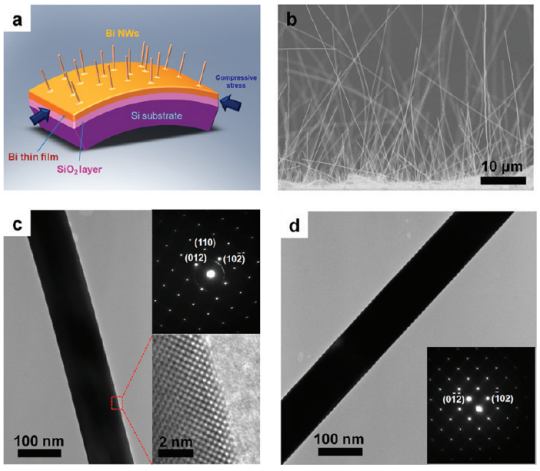

Figure 1. Illustration of growth mechanism and structural characteristic of the single-crystalline Bi nanowires. (a) Illustrated representation of the growth mechanism of Bi nanowires using the OFF–ON method. (b) SEM image of a side view of as-grown Bi nanowires extruding from the surface of the Bi films. (c) Low-magnification TEM image of a single-crystalline Bi nanowire: the SAED pattern (top right) of the nanowire along the [2$\bar{2}$1] zone axis indicates the growth direction of the nanowires is [110], and a high-resolution TEM image (bottom right) of the Bi nanowire shows a perfect single-crystalline material without defects. (d) Low-magnification TEM image of a single-crystalline Bi nanowire: the SAED pattern (bottom right) of the nanowire along the [2$\bar{2}$1] zone axis indicates the growth direction of the nanowires is [$\bar{1}$02].

The presence of the native oxide layer on surface of the nanowires and thermal contact resistance between the Bi nanowire and membrane may cause uncertainty in the thermal conductivity measurement. Bi nanowires are known to have a stable native oxide on the

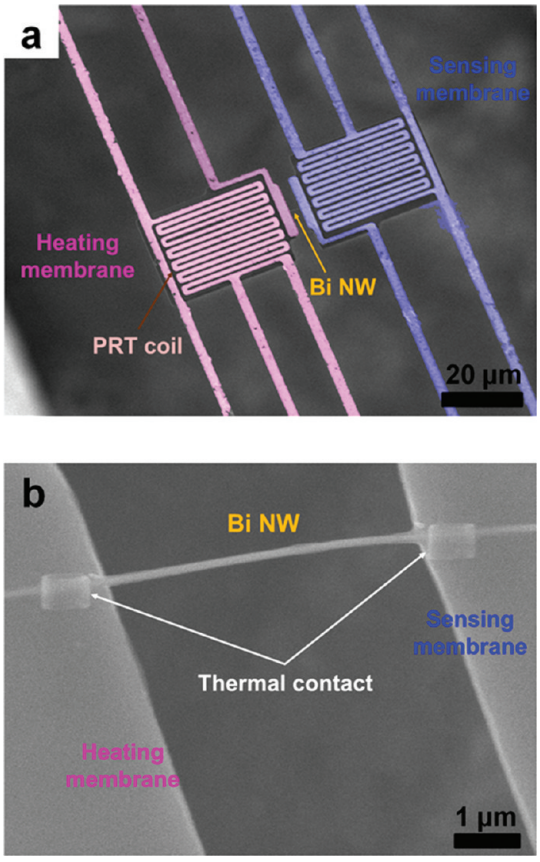

Figure 2. (a) SEM image of the suspended microdevice for measuring the thermal conductivities of the individual Bi nanowires. (b) SEM image of an individual Bi nanowire placed between the heating membrane and sensing membrane. Pt/C composite thermal contact was locally deposited to improve the thermal conduction between the Bi nanowire and membrane using the electron beam of a dual-beam FIB.

surface,[3,19,25] and we also observed that the oxide thickness for the as-grown Bi nanowires is 2−7 nm.[17,26] For a Bi nanowire with a 5 nm thick oxide layer, the thermal conductivity of the nanowire can be underestimated by 6−29% depending on the diameter and length of the nanowires that bridge the membranes. The thermal conduction through the oxide layer was extracted by using a similar calculation proposed by Moore *et al.*[19] Thermal contact resistance between the nanowire and the isothermal suspended membrane on either side is another source of error in thermal conductivity measurement. This error has been hypothesized to be as large as 15% in similar measurements on other nanowires.[19,23,27] Considering the errors due to the native oxide layer from the outer surface of the nanowires and the thermal contact resistance, the measured thermal conductivities of Bi nanowires were corrected in this work similar to Moore *et al.*[19]

It has been reported that the thermal conductivity of bulk Bi depends highly on the crystal orientation.[1] In order to confirm the growth direction on the thermal-conductivity-measured nanowires, HR-TEM coupled

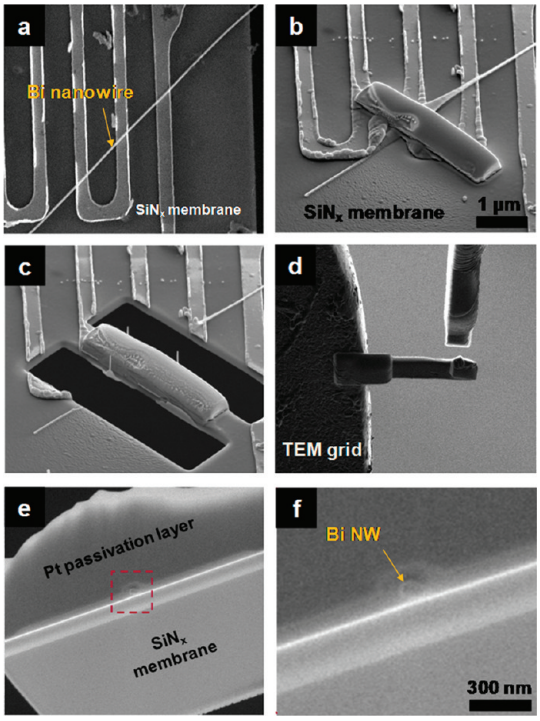

Figure 3. SEM images of sample-preparation process for TEM investigation. (a) Thermal conductivity-measured Bi nanowire (d_w = 98 nm) on the SiN_x membrane. (b) Deposition of Pt passivation layer using electron beam. (c) Cutting the membrane around the TEM sample containing κ-measured Bi nanowires. (d) Attachment of TEM sample to TEM grid using nanomanipulator. (e and f) The fabricated TEM sample contains the thermal-conductivity-measured Bi nanowire.

with selected area electron diffraction was employed after the thermal conductivity measurement was completed. Employing this technique, not only could we corroborate that the nanowires retained their high-quality single-crystalline cores, but we also determined the growth direction of the nanowires postmeasurement. The sample preparation for TEM investigation was performed using the dual-beam FIB system (FEI Quanta 3D FEG). The process for TEM sample preparation is introduced in Figure 3. Care was taken to ensure that only nanowires that survived on both the heating and sensing membranes after measurement were considered. However, the yield was low, as the wires would break during transfer and/or measurement, and hence TEM characterization could not be performed on every measured wire. Thermal conductivity values have only been reported for those wires that survived after measurement.

Figure 4a shows thermal conductivities of individual Bi nanowires at 300 K with different diameters, revealing that the measured thermal conductivities have two separate trends with the diameter of Bi nanowires. From the HR-TEM investigation and the SAED patterns shown in Figure 4c, the growth direction of NW 1 and NW 2 was found to be [$\bar{1}$02], while that of NW 3, NW 4, and NW 5 was [110]. This is consistent with the result

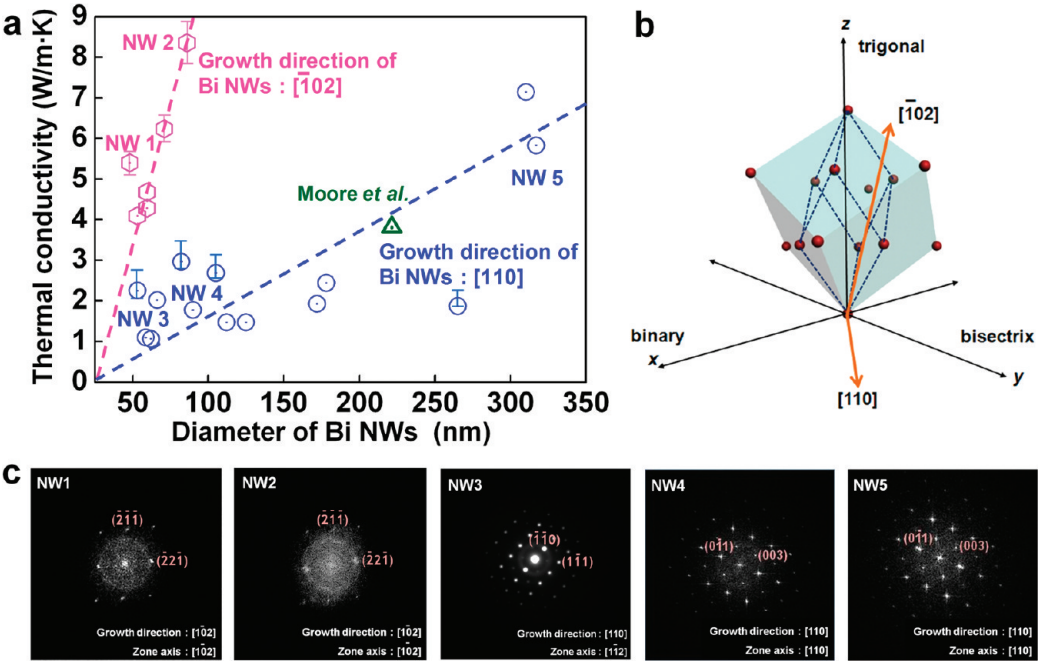

Figure 4. (a) Diameter-dependent thermal conductivity of Bi nanowires with growth directions of [$\bar{1}$02] (pink hexagon) and [110] (blue circle), respectively, at 300 K. The dashed lines represent the linear fit of the measured thermal conductivity for each growth direction of Bi nanowires. The thermal conductivity (green triangle) of Bi nanowire perpendicular to the trigonal axis measured by Moore *et al.* is taken from ref 19. (b) Illustrated representation of the growth direction of Bi nanowires grown by OFF−ON. (c) SAED patterns of the thermal conductivity-measured Bi nanowires. While the ED pattern shows NW 1 and NW 2 were grown along the direction of [$\bar{1}$02], NW 3, NW 4, and NW 5 were grown along the direction of [110].

that as-grown Bi nanowires have two different growth directions, [110] and [$\bar{1}$02].[17] The ring pattern in NW 1 and NW 2 could be attributed to the fact that Pt atoms go into the surface of the Bi nanowire during the process of TEM sample preparation. Gallo *et al.*[1] measured thermal conductivity of single-crystal bulk Bi in directions parallel ($\kappa_{\parallel}$) and perpendicular ($\kappa_{\perp}$) to the trigonal axis and found anisotropy in the thermal conductivity. For example, at 300 K the electronic part dominates thermal conductivity: in the trigonal direction, they measured $\kappa_{\parallel,\mathrm{total}}$ to be 6 W/m·K, with $\kappa_{\parallel,\mathrm{E}}$ about 5 W/m·K; in the perpendicular direction, $\kappa_{\perp,\mathrm{total}}$ was 10 W/m·K, with $\kappa_{\perp,\mathrm{E}}$ about 8 W/m·K.[1] In our case, the nanowire growth directions of [110] and [$\bar{1}$02] are perpendicular and tilted by an angle of 10.85° to the trigonal axis, respectively, as shown in Figure 4b. As shown in Figure 4a, we also observed the anisotropy in thermal conductivities; the thermal conductivities of Bi nanowires with a growth direction of [110] are about 4-fold lower than those of Bi nanowires with growth direction [$\bar{1}$02]. We also included in Figure 4a the thermal conductivity of single-crystalline Bi nanowire measured by Moore *et al.*[19] for reference. The orientation of their Bi nanowire is ⟨1$\bar{2}$0⟩, which is also perpendicular to the trigonal axis, but is different from our growth direction. Further, it can be observed that for a particular growth direction, the thermal conductivity of Bi nanowires decreases with diameter at 300 K. This diameter-dependent thermal conductivity of Bi nanowires suggests that there is enhanced boundary scattering of heat carriers, which are both electrons and phonons.

In bulk Bi,[1] the thermal conductivity along the trigonal direction is lower than that perpendicular to the trigonal direction, and the deviation in thermal conductivities in the two direction is only around 2 W/m·K at 300 K. In contrast, the deviation between [$\bar{1}$02] and [110] directions is around 7 W/m·K at 300 K for 100 nm diameter nanowires. Also, the thermal conductivity in Bi nanowires showed the opposite trend compared with that in bulk; for example, the thermal conductivity along [$\bar{1}$02], *i.e.*, 10.85° from the trigonal direction, is higher than that along [110], *i.e.*, perpendicular to trigonal direction. This may be due to either of the following reasons: (i) There is no report on any transport property let alone thermal conductivity of Bi in this off-axis, *i.e.*, [$\bar{1}$02], direction. From the crystallographic point of view, a tilt of 10.85° from the trigonal direction would cause a considerable difference in transport properties. For example, the nearest atom spacing in the [$\bar{1}$02] direction in bismuth is ~24 Å, while that in the trigonal or [001] direction is ~5.7 Å. We speculate that this could result in a significant difference in the mobility (due to band effective mass), Fermi vector, k_F, and phonon group velocity. (ii) The electron mobility of Bi nanowires in the trigonal [001] direction was observed to be a factor of around 4 times higher than that in the bulk Bi.[17] This enhanced mobility may be caused by the variation in electronic band structure due to the interface between the surface oxide and the Bi cores[28−31] or the reduced Fermi wavevector.[17] Also,

Huber *et al.*[32] studied the contribution of surface states to electronic conductivity in a sub-50 nm single-crystalline Bi nanowire array in the trigonal direction, and they observed that the surface electrons possess high mobility. The enhanced mobility could result in the increased electronic thermal conductivity. However, there is no report on mobility of [$\bar{1}$02] or [110] wires. A detailed experimental study of thermal conductivity as a function of magnetic field would be an exciting direction of proposed research. Also, in terms of the lattice thermal conductivity, there is a theoretical report[33] that a good bulk thermal conductor may not necessarily be a good thermal conductor for nanowires due to alternate contributions to phonon scattering.[8] In any case, more experimental data would resolve this issue.

For the Bi nanowires grown along the direction of [110] with d_w = 117 nm, the corrected thermal conductivity was 2.7 ± 0.1 W/m·K at room temperature, which is higher than the electronic thermal conductivity, κ_E, of ~2.5 W/m·K calculated from the Wiedemann–Franz law using our recently reported electrical conductivity of Bi nanowires with similar diameters.[9] However, for the Bi nanowires grown along the direction of [110] with d_w = 69 nm, the thermal conductivity is as low as 1.1 ± 0.2 W/m·K, which is lower than the κ_E of 1.6 W/m·K estimated from the Wiedemann–Franz law and electrical conductivity of Bi nanowires with similar diameters.[9] Including the inaccurate estimation of diameter due to the native oxide and inevitable thermal contact resistance, the lower values of thermal conductivity could have large errors associated with them. Hence, the variability in the diameter trend should be taken as an additional source of error due to these uncertainties in the thermal conductivity measurement. In spite of considering this uncertainty in the thermal conductivity measurement, our result clearly shows the anisotropy and diameter dependence of thermal conductivity in Bi nanowires for the first time. Gallo *et al.*[1] reported that the total electronic contribution of thermal conductivity, κ_E, for a semimetal such as Bi can be expressed as $\kappa_E = \kappa_e + \kappa_h + \kappa_{he}$ where (1) κ_e is the ordinary thermal conductivity due to electrons only, (2) κ_h is the ordinary thermal conductivity due to holes only, and (3) κ_{he} is the thermal conductivity arising from bipolar diffusion due to the formation of electron–hole pairs. In this case, the electrons still dominate and the high electron mobility direction in bulk Bi corresponds to the low lattice thermal conductivity direction (both parallel to the trigonal axis). Using the electrical conductivity of a Bi nanowire with d_w = 127 nm,[9] the electronic thermal conductivity at room temperature can be estimated to be ~1.9–2.5 W/m·K (assuming $L_{\|} = 2.3 \times 10^{-8}$ W·Ω/K^2 and $L_{\perp} = 3.0 \times 10^{-8}$ W·Ω/K^2),[1] although the growth direction of the nanowire was not known. In both cases, electronic contribution to the total thermal conductivity can be as high as 70% of the total measured thermal conductivity. Thus, both anisotropy and boundary scattering have significant effects on the transport of the heat carriers (electrons, holes, as well as phonons) in the nanowires, but their exact mechanism is not clear. This finding motivates further thermal and electrical study on Bi nanowires with different crystal orientation.

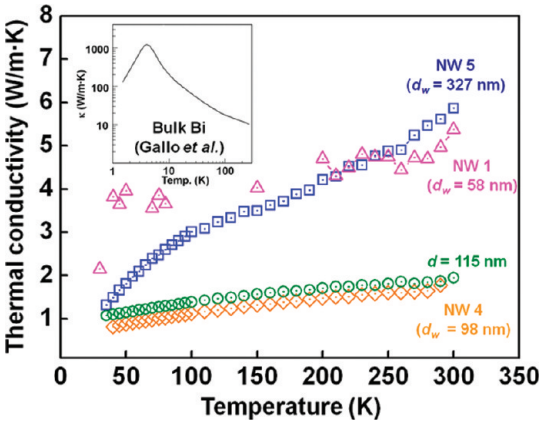

Figure 5. Temperature-dependent thermal conductivities of Bi nanowires with d_w = 58, 98, 115, and 327 nm. The inset shows the temperature-dependent thermal conductivity of bulk Bi (ref 1).

Figure 5 shows the temperature dependence of thermal conductivity for NW 1, NW 4, NW 5, and a Bi nanowire with d_w = 115 nm in the temperature range 40–300 K. The growth direction was confirmed to be [$\bar{1}$02], [110], and [110] for NW 1, 4, and 5, respectively, and is hypothesized to be [110] for the Bi nanowire with d_w = 115 nm based on the anisotropic dependence of κ shown in Figure 4a. The diameters of NW1, NW 4, and NW 5 were 58, 98, and 327 nm, respectively. As shown in Figure 5, the thermal conductivities of the Bi nanowires increase monotonically with increasing temperature, but the actual temperature-dependent behaviors are quite different: NW1 shows a slight increase in κ for T < 200 K but a much sharper one for T > 200 K; NW 4, on the other hand, shows a fairly weak temperature dependence for the entire temperature range. For comparison, the thermal conductivity of bulk Bi (inset of Figure 5) has a sharp peak at the temperature of 4 K,[1] presumably where phonon–phonon *Umklapp* scattering takes over, because phonons are the dominant heat carriers at low temperatures (<200 K)[18] and the Debye temperature of Bi (120 K)[34] is low. The fact that our measured κ monotonically increases with temperature from 40 to 300 K suggests that boundary scattering is significant for both electrons within the entire temperature range and phonons at lower temperature (T < ~200 K), as explained below. At higher temperature, electronic contribution dominates the total thermal conductivity[1] and the lattice contribution is relatively small (<30%). Also, the estimated mean free path of phonons is about 11–14 nm at 300 K; the effect of the boundary on phonon conductivity at this temperature is not significant. However, at lower temperatures the lattice contribution is dominant and the mean free

paths are longer; hence the boundary can scatter phonons more effectively. For instance, below 200 K, lattice contribution is larger than 50% of overall conductivity in bulk Bi and the boundary could affect the phonon mean free path substantially. Thus, one would expect the lattice contribution of a nanowire with a particular diameter to be a constant with temperature due to the boundary scattering since the lattice specific heat above the Debye temperature and the speed of sound are constant.

The electronic contribution to the total thermal conductivity can be estimated from the modified Wiedemann–Franz law as discussed earlier. However, as an additional variable in the case of Bi nanowires, it has been predicted and experimentally verified[3,15,16,25] that there is a semimetallic to semiconducting transition when the diameter of the nanowire is smaller than a certain transitional diameter. According to our electrical measurements of Bi nanowires, the transitional diameter occurs near 63 nm;[9] hence NW1 should be semiconducting. For semiconducting wires, electrical conductivity, σ, increases significantly with temperature at $T > 200$ K, while it is almost flat below 200 K.[9] Thus, below 200 K, the interplay between the almost constant phonon contribution and increasing electronic contribution gives a weakly linear temperature dependence for NW1. Higher than 200 K, the electronic contribution takes over and the temperature dependence is stronger. For the nanowires on the semimetallic side of the transition (NWs 4 and 5 and the 115 nm NW), there is an overall linear temperature dependence due to the constant lattice contribution and an increasing electronic contribution.[9] Therefore, we can attribute the temperature dependence of thermal conductivity to the strong boundary scattering for both electrons and phonons, which is consistent with the observed trend of diameter dependence for thermal conductivity. The details of the temperature dependence, however, can vary for wires with different diameters and crystallographic orientations and merit further investigation, such as concurrent electrical and thermal measurements with quantitative modeling coupled with similar anisotropic considerations as we have done in this work.

CONCLUSION

In summary, we observed the anisotropy in thermal conductivity of single-crystal Bi nanowires grown by the OFF–ON method. The orientation-dependent thermal conductivity of Bi nanowires was analyzed by HR-TEM and SAED investigations for thermal conductivity-measured Bi nanowires. The thermal conductivity of the Bi nanowires with a growth direction of [110], which is perpendicular to the trigonal axis, is about 4-fold lower than that of the Bi nanowires with a growth direction of [$\bar{1}$02], which is 10.85° off the trigonal axis. For a particular growth direction, the thermal conductivity of Bi nanowires scales down with diameter, which indicates the presence of strong boundary scattering of the heat carriers. Our results demonstrate that the growth direction plays a very significant role in charge and energy transport in Bi nanowires, which should be considered when designing thermoelectric devices based on Bi nanowires. Concurrent measurements of both thermal and electrical properties are required to further elucidate the behavior of heat carriers in these high-quality single-crystalline Bi nanowires.

METHODS

Measurement Principle of Thermal Conductivity. Direct current (dc) voltage applied to the Pt coil on the heating membrane generated Joule heat, which increases the temperature of the heating membrane (T_h). The resistance of the Pt coil on the heating membrane (R_h) was measured by a 4-point electrode connected to the Pt coil. A certain amount of heat generated by the Pt coil on the heat membrane was conducted to the sensing membrane through an individual Bi nanowire under thermally steady-state conditions. Due to thermal conductance through the Bi nanowire (G_w), the temperature of the sensing membrane (T_s) also increased, and so did the resistance of the Pt coil on the sensing membrane (R_s). The thermal conductance of a Bi nanowire (G_w) could be obtained from the relation

$$G_w = \frac{P}{\Delta T_h - \Delta T_s}\left(\frac{\Delta T_s}{\Delta T_h + \Delta T_s}\right) \quad (1)$$

where $P = I^2(R_h + R_l/2)$. Here R_l is the total electrical lead resistance of Pt lines that connect to the PRT coil on the heating membrane.

TEM Sample Preparation of Thermal Conductivity-Measured Nanowires. As shown in Figure 3a, the Bi nanowire was first located on the membrane of the suspended microdevices. In order to prevent damage to the Bi nanowire from the Ga^+ ion beam during the TEM sample preparation process, the Pt passivation layer was deposited on the Bi nanowire using an electron beam with a low accelerating voltage of 2 kV and 50 pA (see Figure3b). After deposition of the Pt passivation layer, the Bi nanowire was separated from the membrane using a Ga^+ ion beam and moved to a TEM grid using a nanomanipulator. Then, FIB milling was carried out to reduce the Bi nanowire thickness to 40–50 nm. Finally, to remove the Ga^+ ion-damaged layer from the TEM sample, the sample was cleaned by final milling with a low accelerating voltage of 2 kV and ion current of 48 pA. Figure 3e and f shows the Bi nanowire as embedded between the Pt passivation layer and SiN_x membrane.

Acknowledgment. This work was supported by Priority Research Centers Program (2009-0093823) and by a grant (code 2009K000452) from the Center for Nanostructured Materials Technology under the 21st Century Frontier R&D Programs through the National Research Foundation of Korea (NRF). Majumdar *et al.* acknowledge support from the Office of Basic Energy Science, DOE under Grant DE-AC02-05-CH11231 as well as the National Center for Electron Microscopy, Lawrence Berkeley Lab, which is supported by the U.S. Department of Energy under Contract No. DE-AC02-05CH11231. We thank B. Kavaipatti for useful discussions on the analysis of Bi crystal structure. J.W.R. is thankful for the financial support from the Seoul Science Fellowship.

REFERENCES AND NOTES

1. Gallo, C. F.; Chandrasekhar, B. S.; Sutter, P. H. Transport Properties of Bismuth Single Crystals. *J. Appl. Phys.* **1963,** *34*, 144–152.
2. Liu, K.; Chien, C. L.; Searson, P. C.; Kui, Y. Z. Structural and Magneto-Transport Properties of Electrodeposited Bismuth Nanowires. *Appl. Phys. Lett.* **1998,** *73*, 1436–1438.
3. Zhang, Z. B.; Sun, X. Z.; Dresselhaus, M. S.; Ying, J. Y.; Heremans, J. Electronic Transport Properties of Single-Crystal Bismuth Nanowire Arrays. *Phys. Rev. B* **2000,** *61*, 4850–4861.
4. Abeles, B.; Meiboom, S. Galvanomagnetic Effects in Bismuth. *Phys. Rev.* **1956,** *101*, 544–550.
5. Galt, J. K.; Yager, W. A.; Merritt, F. R.; Cetlin, B. B.; Brailsford, A. D. Cyclotron Absorption in Metallic Bismuth and Its Alloys. *Phys. Rev.* **1959,** *114*, 1396–1413.
6. Chandrasekhar, B. S. The Seebeck Coefficient of Bismuth Single Crystals. *J. Phys. Chem. Solids* **1959,** *11*, 268–273.
7. Shoenberg, D.; Uddin, M. Z. The Magnetic Properties of Bismuth. II. The de Haas-van Alphen Effect. *Proc. R. Soc. London, Ser. A* **1936,** *156*), 701–720.
8. Aubrey, J. E. Cyclotron Resonance in Bismuth. *J. Phys. Chem. Solids* **1961,** *19*), 321–330.
9. Lee, S.; Ham, J.; Jeon, K.; Noh, J. S.; Lee, W. Direct Observation of the Semimetal-to-Semiconductor Transition of Individual Single-Crystal Bismuth Nanowires Grown by On-Film Formation of Nanowires. *Nanotechnology* **2010,** *21*, 405701.
10. Lin, Y. M.; Cronin, S. B.; Ying, J. Y.; Dresselhaus, M. S.; Heremans, J. P. Transport Properties of Bi Nanowire Arrays. *Appl. Phys. Lett.* **2000,** *76*, 3944–3946.
11. White, G. K.; Woods, S. B. The Thermal and Electrical Resistivity of Bismuth and Antimony at Low Temperatures. *Philos. Mag.* **1958,** *3*, 342–359.
12. Eckstein, Y.; Lawson, A. W.; Reneker, D. H. Elastic Constants of Bismuth. *J. Appl. Phys.* **1960,** *31*, 1534–1538.
13. Hicks, L. D.; Dresselhaus, M. S. Thermoelectric Figure of Merit of a One-Dimensional Conductor. *Phys. Rev. B* **1993,** *47*, 16631–16634.
14. Hicks, L. D.; Dresselhaus, M. S. Effect of Quantum-Well Structures on The Thermoelectric Figure of Merit. *Phys. Rev. B* **1993,** *47*, 12727–12731.
15. Lin, Y.-M.; Sun, X.; Dresselhaus, M. S. Theoretical Investigation of Thermoelectric Transport Properties of Cylindrical Bi Nanowires. *Phys. Rev. B* **2000,** *62*, 4610–4623.
16. Sun, X.; Zhang, Z.; Dresselhaus, M. S. Theoretical Modeling of Thermoelectricity in Bi Nanowires. *Appl. Phys. Lett.* **1999,** *74*, 4005–4007.
17. Shim, W.; Ham, J.; Lee, K.-i.; Jeung, W. Y.; Johnson, M.; Lee, W. On-Film Formation of Bi Nanowires with Extraordinary Electron Mobility. *Nano Lett.* **2008,** *9*, 18–22.
18. Heremans, J. P. Low-Dimensional Thermoelectricity. *Acta Phys. Pol., A* **2005,** *108*, 609–634.
19. Moore, A. L.; Pettes, M. T.; Zhou, F.; Shi, L. Thermal Conductivity Suppression in Bismuth Nanowires. *J. Appl. Phys.* **2009,** *106*, 034310–034310-7.
20. Ham, J.; Shim, W.; Kim, D. H.; Lee, S.; Roh, J.; Sohn, S. W.; Oh, K. H.; Voorhees, P. W.; Lee, W. Direct Growth of Compound Semiconductor Nanowires by On-Film Formation of Nanowires: Bismuth Telluride. *Nano Lett.* **2009,** *9*, 2867–2872.
21. Hochbaum, A. I.; Chen, R. K.; Delgado, R. D.; Liang, W. J.; Garnett, E. C.; Najarian, M.; Majumdar, A.; Yang, P. D. Enhanced Thermoelectric Performance of Rough Silicon Nanowires. *Nature* **2008,** *451*, 163–168.
22. Li, D. Y.; Wu, Y. Y.; Kim, P.; Shi, L.; Yang, P. D.; Majumdar, A. Thermal Conductivity of Individual Silicon Nanowires. *Appl. Phys. Lett.* **2003,** *83*, 2934–2936.
23. Shi, L.; Li, D. Y.; Yu, C. H.; Jang, W. Y.; Kim, D.; Yao, Z.; Kim, P.; Majumdar, A. Measuring Thermal and Thermoelectric Properties of One-Dimensional Nanostructures Using a Microfabricated Device. *J. Heat Transfer-T ASME* **2003,** *125*, 881–888.
24. Roh, J. W.; Jang, S. Y.; Kang, J.; Lee, S.; Noh, J. S.; Kim, W.; Park, J.; Lee, W. Size-Dependent Thermal Conductivity of Individual Single-Crystalline PbTe Nanowires. *Appl. Phys. Lett.* **2010,** *96*, 103101–103101−3.
25. Heremans, J.; Thrush, C. M. Thermoelectric Power of Bismuth Nanowires. *Phys. Rev. B* **1999,** *59*, 12579–12583.
26. Shim, W.; Ham, J.; Kim, J.; Lee, W. Shubnikov−de Haas Oscillations in an Individual Single-Crystalline Bismuth Nanowire Grown by On-Film Formation of Nanowires. *Appl. Phys. Lett.* **2009,** *95*, 232107–232107-3.
27. Zhou, F.; Szczech, J.; Pettes, M. T.; Moore, A. L.; Jin, S.; Shi, L. Determination of Transport Properties in Chromium Disilicide Nanowires via Combined Thermoelectric and Structural Characterizations. *Nano Lett.* **2007,** *7*, 1649–1654.
28. Tian, M. L.; Kumar, N.; Chan, M. H. W.; Mallouk, T. E. Evidence of Local Superconductivity in Granular Bi Nanowires Fabricated by Electrodeposition. *Phys. Rev. B* **2008,** *78*, 045417–045417-7.
29. Tian, M. L.; Wang, J.; Zhang, Q.; Kumar, N.; Mallouk, T. E.; Chan, M. H. W. Superconductivity and Quantum Oscillations in Crystalline Bi Nanowire. *Nano Lett.* **2009,** *9*, 3196–3202.
30. Tian, M. L.; Wang, J. G.; Kumar, N.; Han, T. H.; Kobayashi, Y.; Liu, Y.; Mallouk, T. E.; Chan, M. H. W. Observation of Superconductivity in Granular Bi Nanowires Fabricated by Electrodeposition. *Nano Lett.* **2006,** *6*, 2773–2780.
31. Ye, Z. X.; Zhang, H.; Liu, H. D.; Wu, W. H.; Luo, Z. P. Observation of Superconductivity in Single Crystalline Bi Nanowires. *Nanotechnology* **2008,** *19*, 085709.
32. Huber, T. E.; Adeyeye, A.; Nikolaeva, A.; Konopko, L.; Johnson, R. C.; Graf, M. J. *Surface State Band Mobility and Thermopower in Semiconducting Bismuth Nanowires.* http://arxiv.org/abs/1103.1054v3.
33. Mingo, N.; Broido, D. A. Lattice Thermal Conductivity Crossovers in Semiconductor Nanowires. *Phys. Rev. Lett.* **2004,** *93*, 246106–246106-4.
34. DeSorbo, W. Low Temperature Specific Heat of Bismuth and Tungsten. *J. Phys. Chem.* **1958,** *62*, 965–967.